

Magnetic resonance imaging methodology

Ewald Moser · Andreas Stadlbauer ·
Christian Windischberger · Harald H. Quick ·
Mark E. Ladd

Published online: 23 December 2008
© The Author(s) 2008. This article is published with open access at Springerlink.com

Abstract

Introduction Magnetic resonance (MR) methods are non-invasive techniques to provide detailed, multi-parametric information on human anatomy, function and metabolism. Sensitivity, specificity, spatial and temporal resolution may, however, vary depending on hardware (e.g., field strength, gradient strength and speed) and software (optimised measurement protocols and parameters for the various techniques). Furthermore, multi-modality imaging may enhance specificity to better characterise complex disease patterns.

Objective Positron emission tomography (PET) is an interesting, largely complementary modality, which might be combined with MR. Despite obvious advantages, combining these rather different physical methods may also pose challenging problems. At this early stage, it seems that PET quality may be preserved in the magnetic field and, if an adequate detector material is used for the PET, MR sensitivity should not be significantly degraded. Again, this may vary for the different

MR techniques, whereby functional and metabolic MR is more susceptible than standard anatomical imaging.

Discussion Here we provide a short introduction to MR basics and MR techniques, also discussing advantages, artefacts and problems when MR hardware and PET detectors are combined. In addition to references for more detailed descriptions of MR fundamentals and applications, we provide an early outlook on this novel and exciting multi-modality approach to PET/MR.

Keywords Magnetic resonance · Imaging · Spectroscopy · Artefacts · Multi-modality imaging · PET/MR

Introduction

Since magnetic resonance imaging (MRI) entered the clinical arena in the early 1980s, MRI has experienced

E. Moser (✉) · C. Windischberger
MR Center of Excellence, Medical University of Vienna,
Lazarettgasse 14, 1090 Vienna, Austria
e-mail: Ewald.Moser@meduniwien.ac.at

E. Moser · C. Windischberger
Center for Biomedical Engineering and Physics,
Medical University of Vienna,
Währinger Gürtel 18-20, 1090 Vienna, Austria

E. Moser
Department of Diagnostic Radiology,
Medical University of Vienna,
Währinger Gürtel 18-20, 1090 Vienna, Austria

A. Stadlbauer
Department of Neurosurgery,
University of Erlangen—Nuremberg,
Erlangen, Germany

A. Stadlbauer
MR Physics Group, Department of Radiology,
Landeskrankenhaus St. Poelten, Austria

H. H. Quick · M. E. Ladd
Erwin L. Hahn Institute for Magnetic Resonance Imaging,
UNESCO World Cultural Heritage Zollverein,
Arendahls Wiese 199, 45141 Essen, Germany

H. H. Quick · M. E. Ladd
Department of Diagnostic and Interventional Radiology
and Neuroradiology, University Hospital Essen,
Hufelandstrasse 55, 45122 Essen, Germany

dramatic advances associated with an increasing number of clinical applications that, in turn, are driving further technical developments. Shortly after its introduction, MRI became one of the most important diagnostic imaging modalities and continues this role today. This success is due to the inherent characteristics of anatomical MRI, featuring excellent soft tissue contrasts that are based on multiple contrast parameters, the ability to image in oblique orientations and the capability to provide two-dimensional (2D) as well as 3D data. MRI is considered a non-invasive diagnostic imaging modality that generates cross-sectional images of the human body without the use of ionising radiation. The diagnostic importance of MRI is impressively reflected by an ever growing number of MRI scanner installations. Informal market research studies suggest that, today (2008), about 20,000–24,000 MRI systems are installed and operational worldwide. These studies also indicate that about 60–80 million MRI examinations are being performed each year.

As the MR signal depends on a variety of physical tissue parameters, MRI may also provide a broad range of functional information on diffusion, perfusion, flow rates, temperature, magnetic susceptibility, etc. beyond displaying morphologic and structural information. Owing to this spectrum of information, the clinical applications of MRI encompass neurological, psychiatric, abdominal, cardiac, vascular as well as musculoskeletal applications, covering the entire human body. Furthermore, metabolic changes in and around tumours, degenerative brain diseases and accompanying the metabolic syndrome may be visualised using MR spectroscopy (^1H , ^{13}C , ^{31}P) or spectroscopic imaging (^1H , ^{31}P). With the advent of whole-body MR imaging technologies [1], whole-body tumour staging and screening for metastasis has become a viable option today [2–4].

In the context of combined PET and MR imaging, it is important to understand the underlying principles and limitations of both imaging modalities. To provide a basic understanding of MR technology, we shall describe the most important MRI hardware components, their interaction with the human body and some of the most common measurement techniques and parameters that may be varied by the user to obtain the diagnostic information of choice.

We conclude by summarising current knowledge on advantages and challenges in combining the two imaging modalities.

MR hardware

The useable field-of-view (FOV) of an MRI system, in general, is defined by three hardware groups and their

related parameters: (1) the main magnet with its homogeneity over the imaging volume; (2) the gradient system with its linearity over the imaging volume; and (3) the radio-frequency (RF) system with its signal homogeneity and signal sensitivity over the active imaging volume (Fig. 1). Typically, a superconducting magnet provides the high magnetic field strength for producing a strong tissue magnetization and, thus, a basis for high signal-to-noise ratios (SNR). The gradient system plays an important role in signal localization: it must be strong enough to switch the highest possible gradient amplitudes in the shortest possible time to enable rapid data acquisition. Also, it may help to compensate for geometric distortions or susceptibility artefacts. The RF system is charged with receiving the weak MR signal with the very minimum of loss. State-of-the-art magnetic resonance spectroscopy (MRS) and MRI impose very specific demands on these system components of system hardware. Phased-array surface RF coil technology, for example, provides means for shorter acquisition times and enhanced data acquisition flexibility through the use of parallel imaging strategies combined with whole-body surface RF coil coverage of the patient [5].

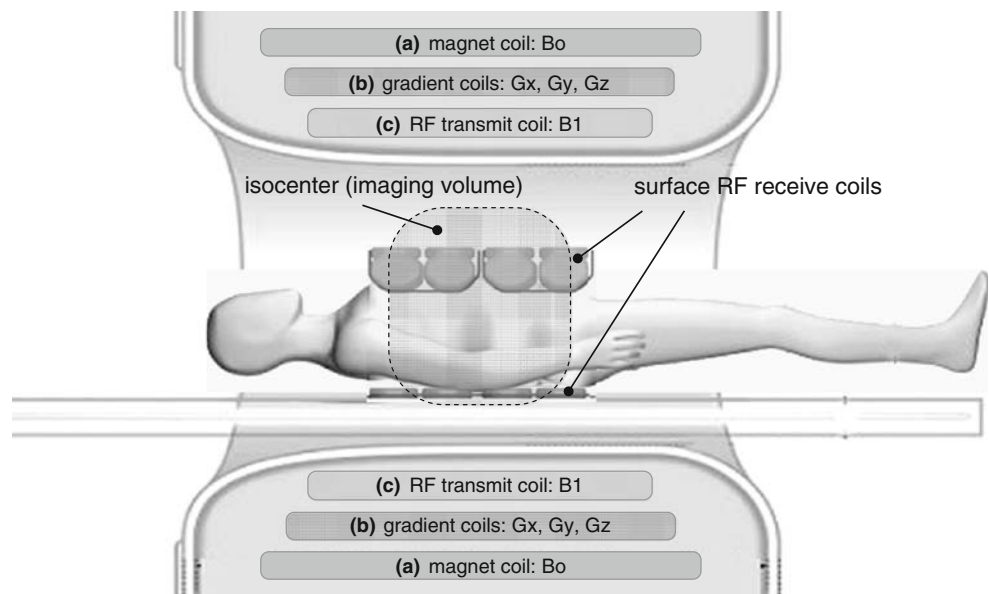
Main magnet—homogeneous static magnetic field

The magnet of a whole-body MR scanner should have a high main magnetic field strength, B_0 , to provide sufficient equilibrium magnetization and therefore a high potential SNR for good image quality. MR systems with field strengths above 1.0 T, or better yet 1.5 T, are currently assumed as the clinical standard and are increasingly being supplemented with 3 T systems in clinical use. Beyond clinical application, a limited but increasing number of 7 T, or even higher field whole-body MR systems have been installed for research investigation in human high-field MR. The homogeneity of the basic magnetic field over the examination volume should be as high as possible to ensure low image distortion and high signal uniformity. Also, the homogenous examination volume should be as large as possible. A cylindrical main magnet with the homogeneous volume centred on the central axis fulfils all these requirements and, therefore, represents the most frequent magnet design today (Fig. 1).

Gradient system—strong, fast and linear (orthogonal) gradient fields

Three orthogonal gradient fields (G_x , G_y , and G_z) are needed for spatial localisation. For performing fast MR imaging, two parameters of the gradient system are critical: a fast gradient slew rate [given in (mT/m/ms)] combined with a high gradient amplitude [given in (mT/m)] are the prerequisites for short repetition (TR) and echo times (TE) and,

Fig. 1 Scheme of a MRI system. (a) magnet coil to produce the homogeneous static magnetic field (B_0) for spin alignment; (b) gradient coils to produce the time-varying gradient fields (G_x , G_y and G_z) for spatial encoding of the MR signals, and (c) transmitter radiofrequency (RF) coil to generate an RF field (B_1) for spin excitation. The MR signal response from the excited spins within the subject is detected by a set of receive-only surface RF coils placed above and below the image volume. Note, the transmit RF coil is optimized for B_1 homogeneity whereas the surface RF coils are optimized for SNR



therefore, for coverage of a large examination volume in the shortest time possible. This can be seen as a fundamental prerequisite for clinically acceptable examination times and for covering large volumes in multi-station or continuously moving table whole-body MRI applications. Ultrafast gradients are also essential in functional (echo-planar) MRI. Fast switching of high-amplitude gradients may, however, also increase the risk of peripheral nerve stimulations [6]. A high degree of gradient linearity over a large volume is required by the gradient system to keep image distortion in and around the image volume to a minimum. These gradient system requirements can be best realized with a cylindrical design to conform to the magnet geometry (Fig. 1).

RF system—homogeneous spin excitation across the body

The radiofrequency (RF) system, in general, consists of a RF transmit coil installed within the MR housing for selective RF excitation of the spins as well as a RF receiver coil system for receiving the weak RF signals leaving the patient. RF excitation of the tissue volume of interest should be as homogeneous as possible. Here, it is important that the RF signal strength for tissue excitation (indicated by the flip angle) remains consistent across the image. Large cylindrical volume transmit RF coils with a conductor geometry similar to a birdcage and fitted within the cylindrical magnet tunnel are typically used (Fig. 1).

On the signal receive side, homogenous RF signal reception over as large an examination volume as possible is desired. However, homogeneity is less important in comparison to signal sensitivity, as inhomogeneous reception intensity only affects the brightness distribution over

the volume, but not the underlying image contrast. Here, as in the transmit case, a whole-body RF coil fitted permanently within the magnet would be advantageous. However, the use of large volume coils limits signal reception and achievable SNR. Hence, various concepts for local RF surface coils have been proposed. Surface RF coils are placed directly over the examination region and receive signals from the immediate vicinity of the coil. The potentially achievable SNR with these coils is much higher than with a volume transmit coil. At the same time, surface coils have a severely restricted sensitivity range. Several coil elements of this type are required to cover larger anatomical regions; they can be combined as phased-array surface coils. Phased-array coils allow optimization of the SNR while extending the region for signal reception (Fig. 2). For imaging of large regions—up to whole-body MR imaging applications—a full set of dedicated local phased-array RF surface coils can be combined on state-of-the-art 1.5 and 3 T MRI systems. A prerequisite for exploring the advantages inherent to this type of coil technology is a large number of RF receivers to which the coil elements can be connected either individually or in groups. This is also a basic prerequisite for the use of parallel imaging techniques where spatial-encoding information of individual RF coil elements can be used to speed up image acquisition.

MR protocol parameters—timing of RF and gradient pulses determines contrast and location

Even the best performing MR hardware mandates MR sequences optimized for particular applications. In this

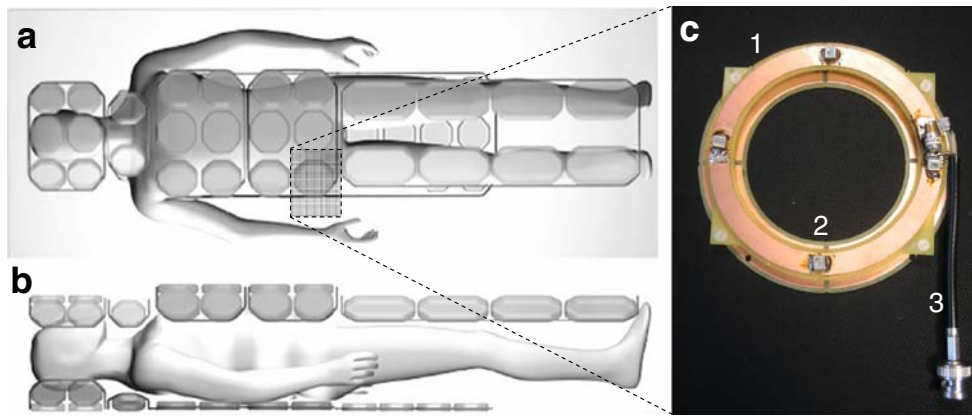


Fig. 2 Schematic representation of radiofrequency (RF) surface coil technology in top view (a) and side view (b). Whole-body coverage of the patient with a full complement of separate RF surface coils in combination with motorized table movement permits whole-body MR imaging applications with relatively high SNR. (c) a close-up of a typical RF receiver single-loop coil element made from copper

conductors (1), ceramic capacitors (2), and coaxial cables (3). Multiple coil elements form a multi-channel RF array coil. For MR signal reception, in a combined MR-PET imaging setup, the RF receiver coils will physically lie between the signal emitting patient and the PET detectors, which potentially could impact the attenuation correction as well as the resulting PET image quality

context, “sequence” refers to a combination of well-defined RF pulses and gradient switching schemes. The specifics of such a pulse sequence determine not only the MR modality (e.g., imaging or spectroscopy), but also contrast and resolution. The combination of a pulse sequence and a particular parameter set (TR, TE, flip angle, matrix size, field-of-view, etc.) defines a protocol. Figure 3 shows two representative examples for MR sequences.

Short RF pulses of a few milliseconds duration are required to excite the nuclear spins. This energy is deposited in the sample and is then irradiated back to a signal-receiving coil. A considerable share of this energy is dissipated into thermal energy and is referred to as the specific absorption rate (SAR). As this process causes

tissue warming, which may be harmful to the patient, SAR limits are constantly controlled throughout an MR scan to ensure compliance with international MR safety guidelines. As indicated by the term “resonance”, spin ensembles will absorb this RF energy effectively only if the transmission frequency is equal to the Larmor frequency of the spins, which scales linearly with the magnetic field strength. For hydrogen nuclei (^1H), this frequency increases from 64 MHz at 1.5 T to 128 MHz at 3 T. It is possible to limit excitation to certain parts of the subject through spatial variation of the magnetic field (via gradients) during RF excitation, thus allowing selection of a volume of interest, as only these irradiated regions will emit RF signals back.

Fig. 3 MR sequence schemes indicating the temporal sequence of RF pulses, gradients and signal acquisition. The spectroscopy sequence (a) consists of a voxel-selection part with three orthogonal slice selections, water suppression and final signal acquisition. The 2D imaging sequence (b) includes initial slice-selective RF excitation, an in-plane phase encoding gradient (before signal acquisition) and a frequency-encoding gradient during signal readout

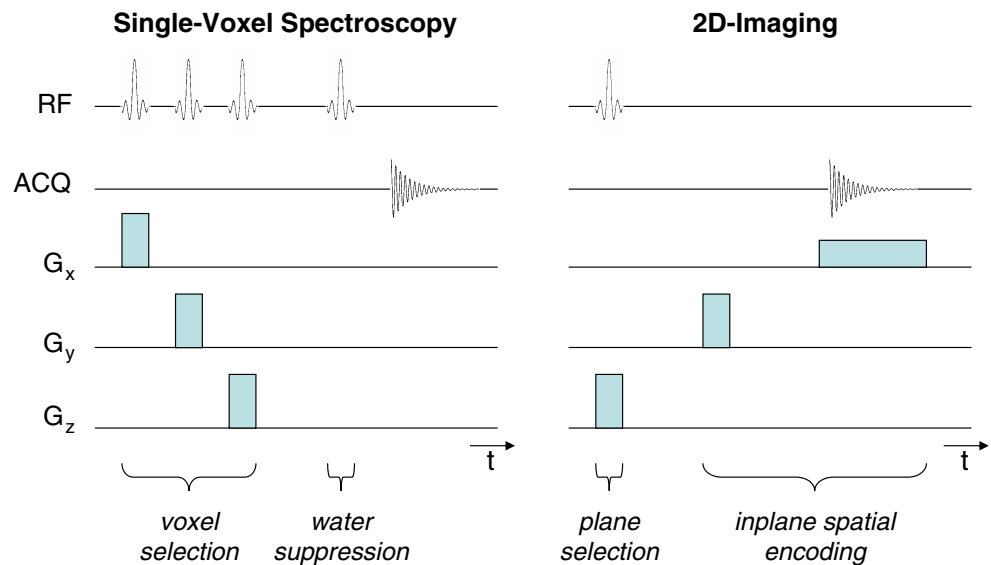


Image contrast, i.e., the relative signal appearance of certain tissues, is determined by tissue properties, sequence type, and sequence parameters (see Fig. 4). Several relaxation constants are used to describe decay and recovery of the MR signal. Most importantly, the longitudinal (or spin-lattice) relaxation time, T_1 , indicates the rate at which the magnetization builds up after an excitation pulse. Tissues with longer T_1 appear hypointense on T_1 -weighted (T_1w) images. The transverse (or spin-spin) relaxation times, T_2 and T_2^* , refer to the rate of signal decay after RF excitation. Tissues with longer T_2 appear hyperintense on T_2w images. The two most important MR parameters governing nearly every MR sequence are echo time (TE) and repetition time (TR). While TE refers to the time between RF excitation and signal acquisition, TR indicates the time between subsequent RF excitations. In combination, TE and TR critically determine the relative contrast weighting of the different tissues. Protocols with short TR and TE will yield T_1w images; long TR

and TE will yield T_2w images. Combining long TR and short TE leads to proton-density-weighted images, where image signal is solely determined by voxel hydrogen content. Acquisitions with short TR and long TE are characterized by very low MR signal strength and are thus not commonly used. The differentiation between T_2w and T_2^*w is primarily determined by the selection of signal refocusing via RF pulses or gradient pulses, as images will generally show T_2w whenever 180° RF pulses (“spin echoes”) are used, but will be T_2^*w when gradient echoes are formed.

In the case of MR spectroscopy, we are interested in metabolite concentrations rather than water content. Hydrogen nuclei bound to metabolites exhibit slightly different Larmor (resonance) frequencies (“chemical shift”) depending on the density of the local chemical environment and, hence, on the density of the electrons. The differences in electron density result in variable shielding of the hydrogen nuclei and, consequently, lead to different resonance frequencies. It is possible to apply a specially designed

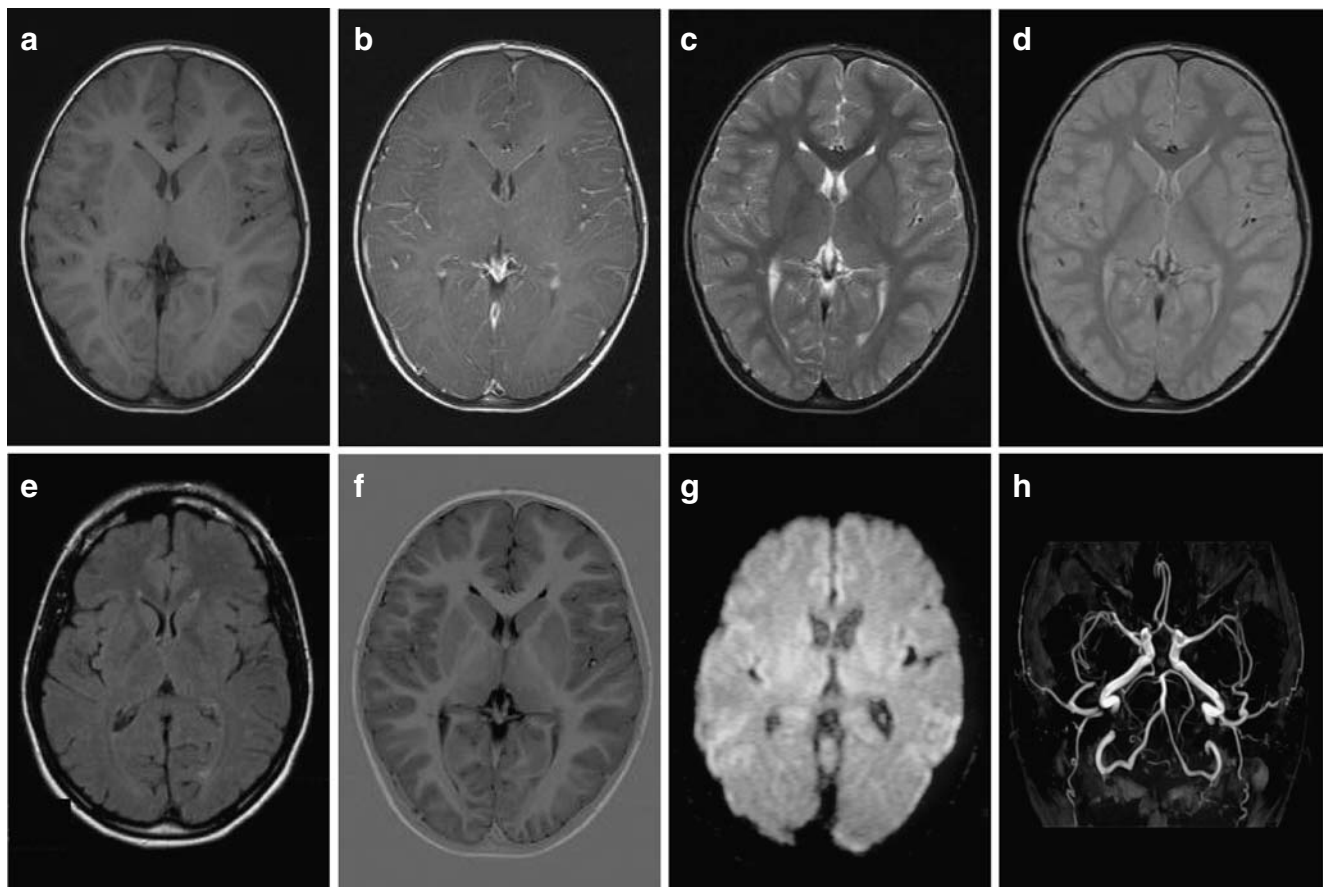


Fig. 4 Choice of multi-parameter soft tissue contrasts available with MRI. Repeated MR imaging of an axial cross-section through the brain of a normal volunteer demonstrates how the soft tissue contrast can be varied simply through the appropriate choice of imaging sequences and corresponding sequence parameters. (a–d) show the basic MRI contrasts: (a) T_1w , (b) T_1w with contrast agent, (c) T_2w ,

(d) proton-density-weighted. (e) and (f) show FLAIR and inversion recovery sequences, respectively. (g) Diffusion-weighted image (DWI) of the brain, and (h) provides a maximum-intensity projection (MIP) of a non-contrast-enhanced 3D time-of-flight (TOF) angiogram of the intracranial vessels

RF pulse to suppress the water signal without altering the metabolite signals. This is required as the mobile water content in human tissue is typically about 50 mol, resulting in a significant water peak, which would mask metabolite peaks detectable by ^1H -MRS (sensitivity in the mM range). Fourier transformation of the acquired MR signal then provides the full spectrum of metabolites in the specified voxel. The duration for single-voxel MRS is just a few minutes, and the spatial resolution is 1 cm^3 or less. In some sequences, referred to as chemical shift imaging (CSI), additional gradients are applied prior to signal acquisition to introduce spatial encoding within the preselected volume, enabling acquisition of spectrums from multiple individual voxels to provide insight into the spatial distribution of the spectroscopic information. This method allows performing MRS with a spatial resolution of 0.1 cm^3 or less [7], which is, however, associated with a significant increase in measurement time up to 1 h or more.

Imaging sequences require additional gradients to introduce spatial encoding (Fig. 3; right). Depending on whether the gradients are applied before or during signal acquisition, they are referred to as phase or readout gradients, respectively. MR signals for imaging sequences are acquired within k -space, which may be regarded as a mathematical model for spin-gradient interactions. The final image is reconstructed after 2D Fourier transformation of the k -space signal. In standard imaging sequences, a single line of k -space is acquired after each RF excitation, i.e., for N image lines (the final image matrix has N pixels along one side), the sequence has to be repeated N times, leading to image acquisition times of up to several minutes. In current ultrafast imaging techniques like echo-planar imaging (EPI) or Turbo Spin Echo (TSE), however, multiple k -space lines or even the entire k -space data are acquired following a single excitation (“single-shot” methods).

MR applications

Structural/anatomical MR imaging

Anatomical imaging by MRI and CT is the clinical standard for all stages in the management of tumour patients, e.g., detection, characterization and staging of the lesion, control of therapeutic response and determination of recurrence. However, it is well known that imaging of the anatomical structure alone suffers from many shortcomings. The evaluation of macroscopic changes in lesions and tissues can lead to a false assessment of the pathologic processes and their progression on the cellular and molecular levels. Furthermore, macroscopic abnormalities commonly are nonspecific and reveal no information about physiological and biological processes.

Functional MRI

This technique uses ultrafast imaging methods, mainly echo-planar imaging (EPI), to collect functional information on blood oxygenation or flow changes [BOLD functional MRI (fMRI)], perfusion or diffusion. fMRI based on the blood oxygen level-dependent (BOLD) effect has been increasingly used to investigate brain function since its introduction in 1990 [8]. It shows a wide field of applications ranging from the investigation of basal and higher brain functions in healthy subjects and animals to pharmacological studies and the preoperative localization of eloquent cortical areas in patients. However, BOLD fMRI assesses changes in the deoxyhemoglobin level, which is associated with hemodynamic response due to changes in neuronal activity. Stimulation of a particular brain area via a defined paradigm leads to a local increase in cerebral blood flow and volume and to a decrease of deoxyhemoglobin content in the capillary bed and the venous-draining vessels. Due to the paramagnetic nature of deoxyhemoglobin, tissue $T2^*$ relaxation time is increased, and subsequently an increased signal intensity on $T2^*w$ images is also observed. In order to observe the BOLD signal change, a $T2^*w$ sequence is needed, typically an echo-planar imaging sequence. MR protocols with a TE approximately equal to $T2^*$ result in maximum BOLD sensitivity upon brain activation.

Compared to functional PET studies, BOLD fMRI experiments show similar spatial resolution and superior temporal resolution. Electrophysiological methods such as EEG and MEG offer better temporal resolution, but EEG has less spatial accuracy and MEG is less available. However, when performing BOLD fMRI, one has to keep in mind the potential confounds, which can occur through drug or disease-induced modulation of physiological events responsible for the generation of the BOLD signal. BOLD fMRI studies are strongly recommended for the preoperative diagnostics of brain tumour patients to delineate functionally important neuronal tissue, which should be preserved during treatment, as well as to obtain information on tumour-induced brain plasticity [10, 11].

Perfusion imaging

This technique is used to investigate differences in the blood supply of lesions and healthy tissue. In principle, noninvasive arterial spin labelling (ASL) can be used to magnetically tag inflowing blood in order to get a direct measurement of organ perfusion [12]. ASL suffers, however, from intrinsically low SNR, and, thus, most applications employ exogenous contrast agents. Dynamic contrast-enhanced MRI (DCE-MRI) techniques require the acquisition of images before, during, and after intravenous

administration of a paramagnetic contrast agent, usually a gadolinium (Gd) chelate bolus [14].

Contrast-enhanced perfusion-weighted MR imaging (PWI) can be performed in two ways. The first is called T1-based perfusion and utilizes the shortening of the T1 relaxation time of tissues by the paramagnetic Gd-based contrast agent. This “T1 effect” is proportional to the amount of contrast media passing through the region under investigation. To observe the changes in the T1 relaxation time, a fast T1-w sequence has to be executed, and the dynamic course of the changes in T1 times is evaluated. T1-based PWI is applied to study the contrast uptake of organs and tissues in the abdomen and thorax (e.g., breast, heart, prostate), usually using a 3D spoiled gradient echo sequence, since this approach allows the acquisition of dynamic information within a breath-hold with good image quality and spatial resolution. It is used to improve tumour diagnosis, evaluate response to therapy, and to detect residual or recurrent tumour. The second PWI method is called T2*-based perfusion and exploits the influence of paramagnetic contrast agent on the local magnetic field which leads to a reduction of the T2* relaxation time in surrounding tissue [14]. A very fast T2*-sensitive sequence has to be performed to measure these changes in the T2* relaxation time, i.e., EPI sequences are commonly applied. During the passage of the contrast agent bolus, the MR signal decreases due to the reduction of T2*, but the signal recovers at least partially after the passage. The differences in occurrence and magnitude of the signal changes are evaluated via an arterial input function (AIF). T2*-based PWI allows for imaging of flow at the capillary level. The measurement of brain perfusion helps to differentiate between acute stroke, hypoglycaemia, hyponatremia, seizure, tumour or subdural hematoma. In acute stroke, for instance, the difference between the diffusion abnormalities measured with DWI and perfusion abnormalities measured with PWI provides a measure of the ischemic penumbra or the brain tissue at risk.

Diffusion-weighted MRI

Diffusion-weighted MRI (DWI) assesses the Brownian motion of water molecules and provides information about tissue structure and intra/extracellular space via the “apparent diffusion coefficient” ADC [15]. DWI shows broad clinical application in diagnosis of acute cerebral infarction, characterization and therapy monitoring of tumours, and differentiation of gliomas from brain abscesses or lymphomas [16]. A DWI sequence detects the signal attenuation due to diffusion of water molecules. The essential parameters for the “diffusivity weighting” are the strength and timing of the diffusion gradients and can be expressed with the “b-factor”. Higher b-factors lead to stronger signal

drop-off in areas with higher diffusion. The observed signal decay can be used to calculate the diffusion properties or ADC.

Depending on the anatomical region, diffusion can occur unrestricted and equal in magnitude in all spatial directions, which is referred to as isotropic diffusion. However, mobility of the water in biological tissue can show a preferred direction governed by structures, e.g., restriction of diffusion by myelinated sheets of nerve fibres, which is referred to as anisotropic diffusion. The DWI method provides information about the magnitude of water diffusion but not about its direction.

Diffusion tensor MR imaging

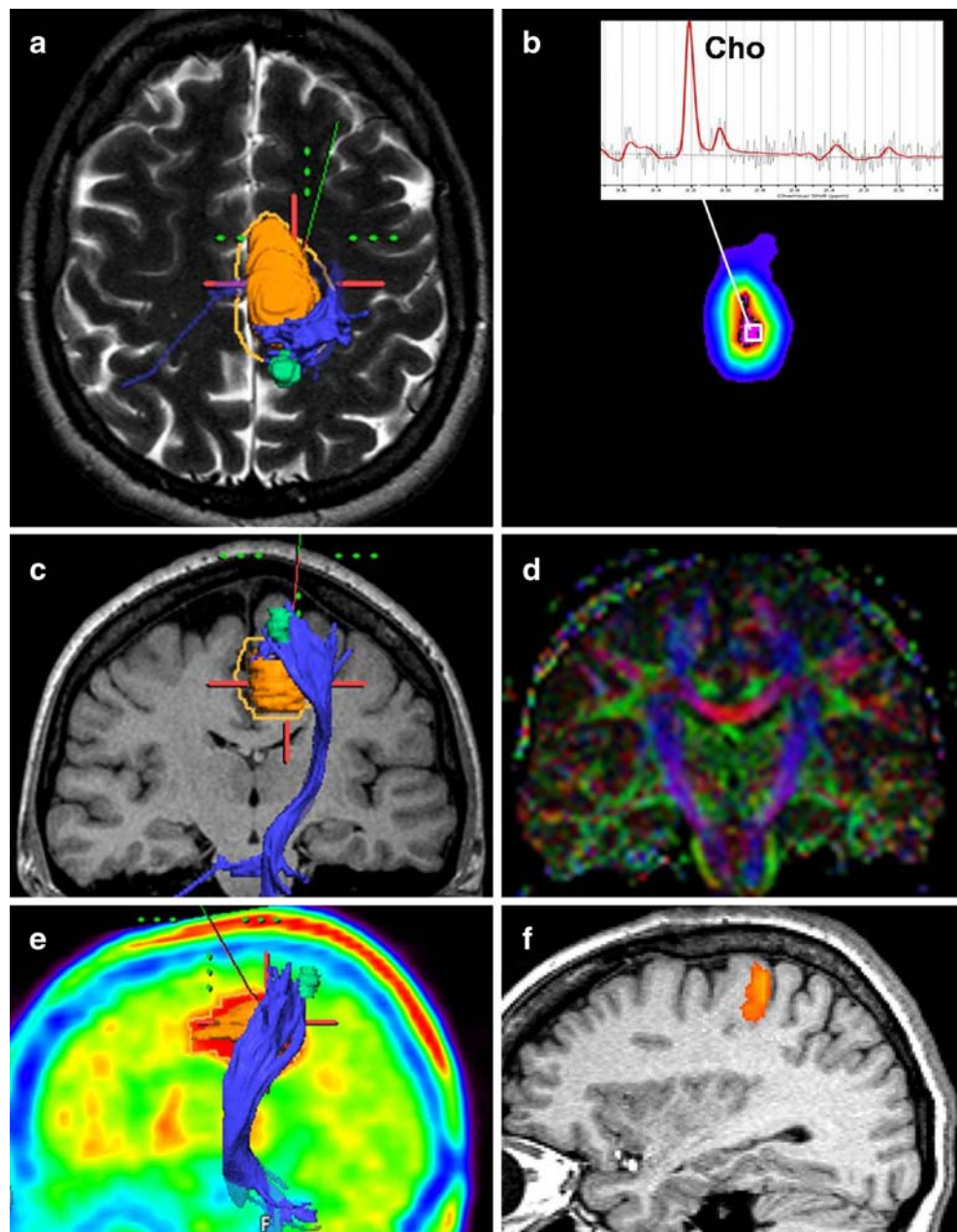
Diffusion tensor MR imaging (DTI) enables the measurement of anisotropic diffusion of water molecules in tissues such as the white brain matter and provides insight into the microstructure of tissues (Fig. 5 D) [17, 18]. DTI shows application in clinical routine for preoperative planning of brain tumour surgery to differentiate peritumoural oedema from tumour border, to assess tumour rim into white-matter tracts, and to visualize and localize the major white-matter tracts (e.g., pyramidal tract; Fig. 5c) intraoperatively [19]. This strategy can help to avoid injuries to normal and/or functionally important brain areas. Application of DWI and DTI is more problematic in regions outside of the brain, e.g., due to increased motion and susceptibility artefacts. However, these methods may provide helpful information regarding the nature and extent of cancer in several organs, which is currently a field of clinical investigations.

Magnetic resonance spectroscopy

MR-based spectroscopy (MRS) is a noninvasive diagnostic tool that allows for the detection of amount and spatial distribution of various molecular compounds, which are involved in the metabolism of pathologic and healthy tissue. In proton MRS (¹H-MRS), the most important metabolites are creatine (Cr), choline (Cho), *N*-acetylacetate (NAA), citrate (Cit), lactate (Lac) and lipids [20]. Unfortunately, no marker specific for cancer and detectable via in vivo MRS exists today. However, one can detect typical metabolic profiles in MRS spectra that provide an indication for cancer [21]. Various studies have assessed the potential of ¹H-MRS to improve diagnosis and prognosis of pathologies in the central nervous system, especially of brain tumours (Fig. 5 B). In recent years, ¹H-MRS has been applied also for diagnosis of other common cancer types such as prostate and breast carcinoma [22, 23].

3D ¹H-MRS sequences with a spatial resolutions comparable to that of PET [7] suffer from low signal-to-

Fig. 5 Multi-modality imaging of a 39-year-old female patient with a glioblastoma multiforme IV. **(a)** axial T2w MR with manually segmented tumour volume (orange), pyramidal tract (blue) and volume of BOLD activation based on foot movement (green), **(b)** segmented map of Cho/NAA and a spectrum of the central tumour with a Cho peak, **(c)** coronal T1w MR fused with the volumes from **(a, d)** colour-coded coronal image of fractional anisotropy (FA) as a result of a DTI experiment (blue feet-head, red left-right, green anterior-posterior), and **e** sagittal ^{18}F -FET PET fused with the volumes from **(a)**



noise and have the drawback of long acquisition times. The application of so-called parallel imaging techniques (e.g., SENSE) [24] is a strategy to overcome this problem. However, ^1H -MRS is very sensitive to susceptibility artefacts, which excludes the use of this method in patients with subcranial, frontobasal, temporal, etc. lesion locations or in patients after surgery. Unfortunately, these problems are more evident at higher magnetic field strength.

The sensitivity of ^1H -MRS is in the range of millimolars. Positron-emitting analogues of molecules, which are involved in metabolic processes, can be detected with PET in picomolar concentrations. A wide variety of PET tracers have been developed to target the transport and

metabolism of glucose (FDG) and amino acids (^{18}F -fluorothymidine or ^{18}F -fluoroethyltyrosine; Fig. 5 E). On the other hand, ^1H -MRS may be performed with any modern MRI system without the need for exogenous tracers, while the availability of PET is still limited in part due to the substantial infrastructure required for tracer production.

Whole-body tumour staging

Whole-body tumour staging utilizing MRI has now become feasible due to several technical innovations: whole-body coverage with RF surface coils (Fig. 2), multiple RF receiver channels, extended and fast table translation. Prior

to these innovations, MR has been limited to examination of a single organ region, which fit within the homogeneous FOV of the magnet. It is now possible to perform complete TNM-staging using multiple pulse sequence 15–30 min, depending on the exact protocol and image resolution [3, 25].

To ensure the highest diagnostic accuracy, paramagnetic contrast agents are used. The logistics of contrast administration for examination of multiple body regions is a major consideration in the development of clinical protocols. Here, the cumulative dose is limited, and dynamic contrast diminishes after multiple injections due to contrast uptake in the surrounding tissue. Figure 6 shows an example of a state-of-the-art oncology staging protocol, which enables the acquisition of dynamic contrast agent

uptake in the abdominal organs and the evaluation of steady-state contrast enhancement of brain and other lesions.

SNR/artefacts

Many practical imaging decisions are based on a compromise between the SNR and the time available for image acquisition, as the SNR increases with the square root of acquisition time. SNR also increases approximately linearly with the main magnetic field strength [26]. A higher SNR translates into improved spatial resolution or reduced scan times. Any modification of the MR environment, for example, by adding PET components to the MR, must avoid significant degradation of the SNR.

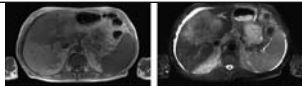
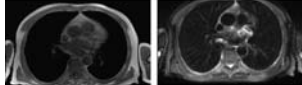
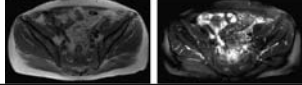
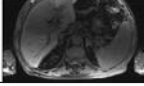
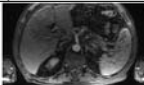
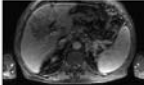
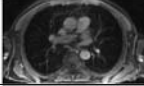
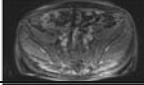
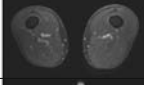
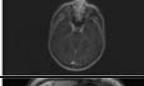
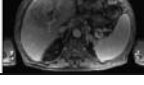
Anatomical Region	Sequence Type	Duration	
abdomen	T1-w 2D spoiled GE T2-w 2D single-shot SE	25 s (breathhold) 25 s (breathhold)	
thorax	T1-w 2D spoiled GE T2-w 2D single-shot SE	25 s (breathhold) 25 s (breathhold)	
pelvis	T1-w 2D spoiled GE T2-w 2D single-shot SE	25 s (breathhold) 25 s (breathhold)	
abdomen	T1-w 3D spoiled GE with FS (pre-CA)	22 s (breathhold)	
intravenous bolus injection of single dose 0.5M Gd CA (10ml for 50kg BW)			
abdomen	T1-w 3D spoiled GE with FS (arterial CA phase)	22 s (breathhold)	
abdomen	T1-w 3D spoiled GE with FS (portal venous CA phase)	22 s (breathhold)	
thorax	T1-w 3D spoiled GE with FS (steady-state CA phase)	22 s (breathhold)	
pelvis	T1-w 3D spoiled GE with FS (steady-state CA phase)	22 s (breathhold)	
upper legs	T1-w 3D spoiled GE with FS (steady-state CA phase)	22 s	
head	T1-w 3D spoiled GE with FS (steady-state CA phase)	22 s	
abdomen	T1-w 3D spoiled GE with FS (late venous CA phase)	22 s (breathhold)	
ca. 6 min. total imaging time ca. 15 min. total in-room time			

Fig. 6 Clinical examination protocol for whole-body MRI oncologic staging. Contrast logistics place constraints on the timing and order of particular imaging regions, leading to multiple table movements

between imaging regions. These constraints may be in conflict with the needs of sequential PET imaging. (w weighted, GE gradient echo, SE spin echo, FS fat saturation, CA contrast agent, BW body weight)

Several other sources of image quality degradation must also be avoided [27, 28]. Due to the switching gradient magnetic fields and also due to the high-frequency RF fields, currents can be induced in electrically conducting structures, which can lead to signal dropouts and other artefacts. In addition to having low conductivity, all materials in the imaging FOV should also provide a good magnetic susceptibility (χ) match to either air ($\chi \approx 0$) or to the human tissue that is slightly diamagnetic ($\chi \approx -9 \times 10^{-6}$). Metallic materials which have a different susceptibility will cause distortion in the homogeneity of the main magnetic field, leading to geometric distortion of the image due to false mapping of signal. The accompanying intra-voxel phase dispersion may lead to signal dropout (Fig. 7 A).

Furthermore, a MR system is a very sensitive radio receiver tuned to a frequency band centred around 64 MHz at 1.5T and 128 MHz at 3T (for hydrogen protons and less for other nuclei). Any electronic noise at the reception frequency will cause banding artefacts in the images (Fig. 7b), or elevated noise levels. Common sources of such noise are any active electronics, and all electronics must be properly shielded to avoid interference.

MR imaging is also susceptible to some artefacts which may hamper proper co-registration of images with an independent imaging modality such as PET. These imperfections may be of particular consequence for

attenuation correction algorithms based on the MR data, which rely on proper overlay of the complementary image sets.

First, since many MR imaging sequences are rather slow compared to physiological processes, cardiac and breathing motion often contaminate the images (Fig. 7d), which is a familiar problem from PET/CT imaging. In addition, signal localization in MR imaging is achieved by the application of ideally linear gradients in the magnetic field. However, due to hardware limitations and the potential of peripheral nerve stimulation during very fast imaging, a certain amount of nonlinearity is acceptable in the periphery of the nominal imaging FOV. As a consequence, the signal is mapped to the incorrect location in the reconstructed image, up to several centimetres at the periphery of large FOVs [29] (Fig. 7c). Although correction algorithms are available, they are typically limited to in plane correction, and they cannot account for extreme nonlinearities.

Finally, it is common in MR imaging to undersample the raw data space in order to save acquisition time. Undersampling in the spacing of raw data lines in the phase-encoding direction leads to fold-over artefacts if the effective FOV is smaller than the object being imaged. This strategy is followed when the imaging region is of limited extent, such as in cardiac exams (Fig. 7e).

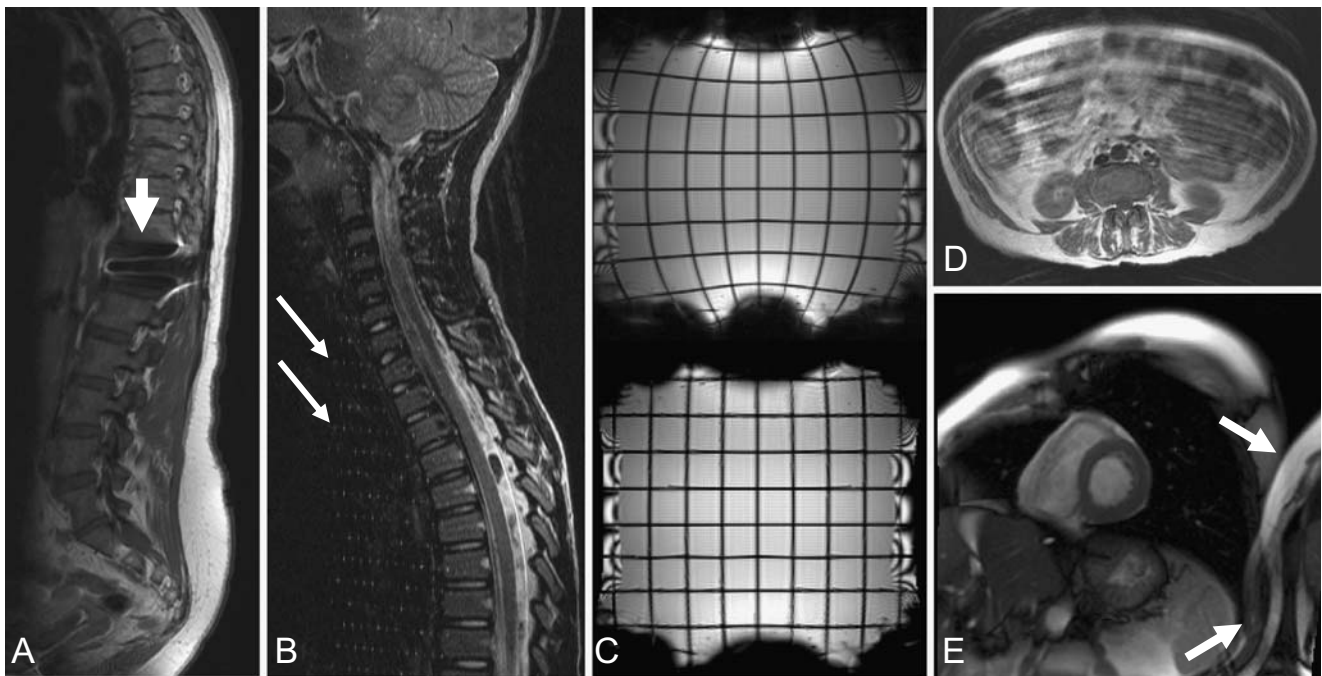


Fig. 7 Characteristic image distortions in MR. (a) Susceptibility artefact (arrow) from a metal fixation screw in the spine; (b) RF artefact (arrows) from improper sealing of the door to the MR examination room; (c) gradient nonlinearity leading to spatial distortion in a $400 \times 400 \text{ mm}^2$ FOV (top); after software correction

(bottom). (d) abdominal respiratory motion artefacts in the anterior-to-posterior phase-encoding direction; and (e) fold-over artefact (arrows) in the left-to-right phase-encoding direction of a short-axis cardiac view

Obviously, MR-based attenuation correction based on images suffering from fold-over distortions will be quite challenging.

Discussion and outlook

MR imaging has experienced rapid growth since its introduction into clinical routine in the 1980s. Much of this growth is due to the enormous flexibility of the method and the large variation in tissue contrasts that can be achieved to reveal pathology and detailed structural and biochemical information. The clinical synergies that can be achieved by a multimodality approach [30] combining simultaneous or quasi-simultaneous PET and MRI in humans are still unknown, although first results from animal studies are rather promising [32]. To achieve maximum impact, the strengths and weaknesses of both imaging techniques need to be considered and strategies developed, which account for complementary imaging properties. The following concerns come to mind:

- (a) high-resolution MR images that complement PET should be the least affected by a PET insert, in particular in the brain, as very strong gradient inserts (≥ 100 mT/m) may be used to compensate for geometric distortions or susceptibility artefacts,
- (b) functional MRI of the brain (i.e., BOLD fMRI, perfusion, diffusion) using EPI or spiral imaging would be very sensitive to SNR or CNR losses caused, e.g., by PET inserts. This may be compensated, in part, by longer measurement times or higher field strengths,
- (c) the most serious problems are to be expected in whole-body PET/MR at high field strengths. Limitations are due to inherent MR problems such as reduced homogeneity in large FOVs and dielectric losses, leading to signal losses, which would be further exacerbated by PET components that reduce SNR and/or increase susceptibility differences,
- (d) user-friendly 3D doctors, finally, integrated models will need to be developed and tested in order to better understand the origins of complex diseases.

Assuming these challenges can be addressed, the question still remains, how a practical examination could be performed on a combined PET/MR tomograph. Even if the hardware enables simultaneous artefact-free data acquisition for both modalities, would it make sense? Individual MR sequences for imaging the head often last minutes. If the longitudinal FOV of the PET is sufficient to cover the brain, then several individual MR contrasts could be acquired, while counts are continuously collected for reconstruction of a single, low-noise PET dataset. For

imaging outside the brain with combined PET/MR, a similar strategy to brain imaging might be pursued if the area of interest is limited to a single organ.

For examinations requiring extended FOV coverage, on the other hand, the examination logistics may not be as straightforward. For most oncologic staging applications, multiple longitudinal FOVs must be sampled. The longitudinal FOV of most MR scanners is 40–50 cm, exceeding typical PET FOVs by a factor of 2–3. Even if the PET FOV can be extended to cover a larger extent, the acquisition of MR contrast agent dynamics may force movement between individual table positions every 20–25 s. PET data sampling will have to be repeatedly stopped and resumed when the table returns to the appropriate position. Current PET/CT implementations subdivide the problem into two sequential acquisitions: first CT then PET. This will most likely not be possible in PET/MR imaging, as there will be periods of “slow” MR data acquisition where it would be inefficient not to acquire PET counts.

Regardless of whether simultaneous PET/MR ultimately makes its way into clinical routine, the efforts to integrate these two technologies will surely expand our understanding how to best exploit the complementary strengths of these two powerful imaging modalities. The role of both PET and MR in medical diagnostics, whether combined or individually, will continue to expand.

Conflict of interest There are no conflicts of interest for any of the authors.

Open Access This article is distributed under the terms of the Creative Commons Attribution Noncommercial License which permits any noncommercial use, distribution, and reproduction in any medium, provided the original author(s) and source are credited.

References

1. Ruehm SG, Goyen M, Barkhausen J, Kroger K, Bosk S, Ladd ME, et al. Rapid magnetic resonance angiography for detection of atherosclerosis. *Lancet* 2001;357:1086–91.
2. Lauenstein TC, Goehde SC, Herborn CU, Treder W, Ruehm SG, Debatin JF, et al. Three-dimensional volumetric interpolated breath-hold MR imaging for whole-body tumor staging in less than 15 minutes: a feasibility study. *AJR* 2002;179:445–9.
3. Lauenstein TC, Goehde SC, Herborn CU, Goyen M, Oberhoff C, Debatin JF, et al. Whole-body MR imaging: evaluation of patients for metastases. *Radiology* 2004;233:139–48.
4. Antoch G, Vogt FM, Freudenberg LS, Nazaradeh F, Goehde SC, Barkhausen J, et al. Whole-body dual-modality PET/CT and whole-body MRI for tumor staging in oncology. *JAMA* 2003;290:3199–206.
5. Larkman DJ, Nunes RG. Parallel magnetic resonance imaging. *Physics in medicine and biology* 2007;52:R15–55.

6. Schaefer DJ, Bourland JD, Nyenhuis JA. Review of patient safety in time-varying gradient fields. *J Magn Reson Imaging* 2000;12:20–9.
7. Gruber S, Mlynarik V, Moser E. High-resolution 3D proton spectroscopic imaging of the human brain at 3 T: SNR issues and application for anatomy-matched voxel sizes. *Magn Reson Med* 2003;49:299–306.
8. Ogawa S, Lee TM, Kay AR, Tank DW. Brain magnetic resonance imaging with contrast dependent on blood oxygenation. *Proceedings of the National Academy of Sciences of the United States of America* 1990;87:9868–72.
9. Norris DG. Principles of magnetic resonance assessment of brain function. *J Magn Reson Imaging* 2006;23:794–807.
10. Beisteiner R, Lanzenberger R, Novak K, Edward V, Windischberger C, Erdler M, et al. Improvement of presurgical patient evaluation by generation of functional magnetic resonance maps. *Neurosci Lett* 2000;290:13–16.
11. Vlieger EJ, Majoie CB, Leenstra S, Den Heeten GJ. Functional magnetic resonance imaging for neurosurgical planning in neuro-oncology. *Europ Radiol* 2004;14:1143–53.
12. Detre JA, Alsop DC. Perfusion magnetic resonance imaging with continuous arterial spin labeling: methods and clinical applications in the central nervous system. *European journal of radiology* 1999;30:115–24.
13. Hylton N. Dynamic contrast-enhanced magnetic resonance imaging as an imaging biomarker. *J Clin Oncol* 2006;24:3293–8.
14. Roberts TP, Mikulis D. Neuro MR: principles. *J Magn Reson Imaging* 2007;26:823–37.
15. Le Bihan D, Poupon C, Amadon A, Lethimonnier F. Artifacts and pitfalls in diffusion MRI. *J Magn Reson Imaging* 2006;24:478–88.
16. Chenevert TL, Meyer CR, Moffat BA, Rehemtulla A, Mukherji SK, Gebarski SS, et al. Diffusion MRI: a new strategy for assessment of cancer therapeutic efficacy. *Mol Imaging* 2002;1:336–43.
17. Le Bihan D, Mangin JF, Poupon C, Clark CA, Pappata S, Molko N, et al. Diffusion tensor imaging: concepts and applications. *J Magn Reson Imaging* 2001;13:534–46.
18. Stadlbauer A, Prante O, Nimsky C, Salomonowitz E, Buchfelder M, Kuwert T, et al. Metabolic imaging of cerebral gliomas: spatial correlation of changes in *O*-(2-18F-fluoroethyl)-L-tyrosine PET and proton magnetic resonance spectroscopic imaging. *J Nucl Med* 2008;49:721–9.
19. Cruz LC Jr., Sorensen AG. Diffusion tensor magnetic resonance imaging of brain tumors. *Magnetic resonance imaging clinics of North America* 2006;14:183–202.
20. Mountford C, Lean C, Malycha P, Russell P. Proton spectroscopy provides accurate pathology on biopsy and in vivo. *J Magn Reson Imaging* 2006;24:459–77.
21. Sorensen AG. Magnetic resonance as a cancer imaging biomarker. *J Clin Oncol* 2006;24:3274–81.
22. Sharma U, Mehta A, Seenu V, Jagannathan NR. Biochemical characterization of metastatic lymph nodes of breast cancer patients by in vitro ¹H magnetic resonance spectroscopy: a pilot study. *Magnetic resonance imaging* 2004;22:697–706.
23. Kurhanewicz J, Vigneron DB, Nelson SJ. Three-dimensional magnetic resonance spectroscopic imaging of brain and prostate cancer. *Neoplasia* (New York, NY 2000;2:166–89.
24. Dydak U, Weiger M, Pruessmann KP, Meier D, Boesiger P. Sensitivity-encoded spectroscopic imaging. *Magn Reson Med* 2001;46:713–22.
25. Schmidt GP, Haug AR, Schoenberg SO, Reiser MF. Whole-body MRI and PET-CT in the management of cancer patients. *Europ Radiol* 2006;16:1216–25.
26. Haacke EM, Brown RW, Thompson MR, Venkatesan R. *Magnetic resonance imaging: physical principles and sequence design*. New York: John Wiley & Sons; ; 1999.
27. Stadler A, Schima W, Ba-Ssalamah A, Kettenbach J, Eisenhuber E. Artifacts in body MR imaging: their appearance and how to eliminate them. *Europ Radiol* 2007;17:1242–55.
28. Bernstein MA, Huston J 3rd, Ward HA. Imaging artifacts at 3.0T. *J Magn Reson Imaging* 2006;24:735–46.
29. Wang D, Strugnell W, Cowin G, Doddrell DM, Slaughter R. Geometric distortion in clinical MRI systems Part I: Evaluation using a 3D phantom. *Magnetic resonance imaging* 2004;22:1211–21.
30. Gerstl F, Windischberger C, Mitterhauser M, Wadsak W, Holik A, Kletter K, et al. Multimodal imaging of human early visual cortex by combining functional and molecular measurements with fMRI and PET. *NeuroImage* 2008;41:204–11.
31. Pichler BJ, Wehrl HF, Kolb A, Judenhofer MS. Positron emission tomography/magnetic resonance imaging: the next generation of multi-modality imaging? *Seminars in nuclear medicine* 2008; 38:199–208.
32. Judenhofer MS, Wehrl HF, Newport DF, Catana C, Siegel SB, Becker M, et al. Simultaneous PET-MRI: a new approach for functional and morphological imaging. *Nature medicine* 2008;14:459–65.